World Scientific
www.worldscientific.com

INTERFERENCE IN FAR-FIELD RADIATION OF EVANESCENT FIELDS

R. CORTES* and V. COELLO

Unidad Monterrey,
Centro de Investigación Científica y de Educación Superior de Ensenada,
Alianza Sur 203, Autopista al Aeropuerto Km 10, Parque PIIT,
Apodaca, N.L., C. P. 66600, México
*rcortes@cicese.mx

P. SEGOVIA and C. GARCÍA

Doctorado en Ingeniería Física Industrial,
Facultad de Ciencias Físico-Matemáticas, UANL,
Pedro de Alba S/N Ciudad Universitaria,
San Nicolás de los Garza, N.L., C. P. 66451, México

J. M. MERLO and J. F. AGUILAR

Tecnológico de Monterrey, Campus Puebla,
Vía Atlixcayotl 2301, San Andrés Cholula,
Puebla, C. P. 72800, México

We investigate experimentally the interference in far-field radiation of two contra-propagating evanescent fields using a conventional optical microscope. A laser beam illuminates a glass-air interface under total internal reflection condition and through the proper setup a double evanescent illumination was produced. The evanescent fields radiate from the surface into the far field domain due to small surface scatterers. Thus, coherent interference is produced in the far field region which is correlated with the relative positions of the evanescent illumination sources. Finally, the above described could be considered as a device for high accuracy micro-scale measurements as well as a direct visualization method of evanescent phenomena.

Keywords: Evanescent waves; optical interference; optical microscopy.

1. Introduction

Evanescent waves (EWs) are electromagnetic modes with an intensity that exhibit exponential decay with distance from the boundary at which the wave was formed.[1] The described phenomenon was first recognized by Newton in a well-known experiment.[2] Nowadays, the effect is the basis of several important technologies including guided optics, waveguides and fiber optic couplers,[3] internal reflection spectroscopy,[4] and near-field optical microscopy,[5] among others. In a general form, the fundamentals of such applications are found in the EW coupling.[1] Evanescent wave coupling, as near field interaction, is one of the concerns in electromagnetic theory research[6−10] and plays a major role in the theoretical explanation of extraordinary optical transmission.[11] The physical

---

*Corresponding author.

mechanisms that couple EWs into propagating waves have been explained in several works.[12,13] In this context, a rounded steel tip ($\approx 50\,\mu$m), acting as a probe, was used to couple a local evanescent field into propagating waves. The method was reported as the first direct experimental evidence of the presence of an evanescent wave.[14] The technique provided a strong scattering that could be collected by a microscope objective or even observed by the eye.

Using similar principles, a classical objective microscope was also reported as a tool for direct visualization method of surface plasmon polariton (SPP) scattering.[15] Due to their electromagnetic nature, one can infer that EWs can diffract, reflect, and interfere. Evanescent wave interference has been used as an excellent method for calibration of near-field optical microscopy.[16] More recently, evanescent wave interference was applied to produce nanoscale photolithography.[17] Here, using a conventional optical microscope, we report on the observation of EW interference patterns in the far-field domain. Evanescent fields were coupled into far-field radiation using small defects (scatterers) located at the surface where they were created. Furthermore, we show the ability to use conventional far field optical microscopy, in combination with evanescent interferometry, to perform high-accuracy length measurements at the micro and nano-scale. Finally, in order to extend the capabilities of the method, the diffraction pattern of a circular aperture illuminated with coherent evanescent wave scattering was illustrated. The technique offers an easy implementation and relative low-cost and it can also be conceptualized for pedagogical purposes of evanescent wave phenomena. We would like to emphasize that all the interference and diffraction effects presented here are due to coherent inelastic (out of the plane) EW scattering.

2. Experimental Techniques

The experimental setup is schematically described in Fig. 1. Light beam from a He−Ne laser (633 nm) is used in the experiments. The critical angle of the right angle prism is measured as $43.3°$. We have created an evanescent field by simply directing the laser beam perpendicular to a side face of the glass prism i.e. beyond the critical angle where total internal reflection (TIR) occurs. In this configuration, internal reflection causes the light to be reflected
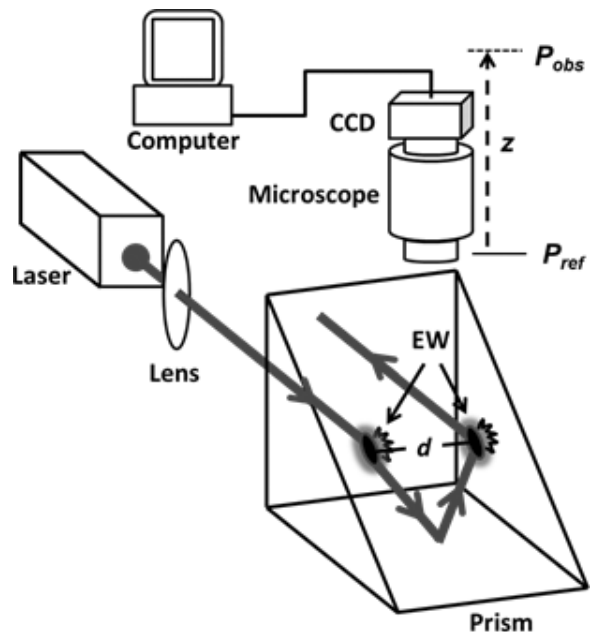

Fig. 1.   Setup used for direct visualization of evanescent wave scattering.

back to where it originated, therefore creating a second (counter-propagating) evanescent field. By gently rotating the prism (in the beam propagation plane), double evanescent illuminations that do not overlap each other can be achieved (Fig. 1). Due to surface roughness, the EWs are partly converted into propagating waves which can be detected in the far field. The propagating components are collected with an optical microscope ($40\times$, working distance 80 mm) and finally recorded with a CCD camera. Young's interference fringes are observed resulting from the light scattered from the two evanescent fields. In Young's original experiments, sunlight, passing through two slits, produced a pattern of closely-spaced dark and bright fringes on another screen. Using the paraxial approximation, the bright fringes occurs when,

$$d \approx \frac{z\lambda}{\Lambda}, \tag{1}$$

where λ is the wavelength of the light, d is the separation of the slits, Λ is the distance between the bands of light and the central maximum (also called fringe period), z is the distance from the slits to the screen center point. This approximation depends on certain conditions, most importantly that $z \gg d$ and the fringes would not be of high orders. Bearing this fact in

1 mind, it is possible to work out the separation distance
2 between the counter-propagating fields using this
3 equation and the abovementioned optical setup. In
4 our case, d becomes the separation between the
5 counter-propagating evanescent fields, and z is the
6 distance from reference position, P_{ref} to an obser-
7 vation position, P_{obs} (Fig. 1). Here, P_{ref} is the position,
8 at which the sharpest of each individual spots image
9 can be visualized, and P_{obs} is the position, at which a
10 sharp interference pattern can be observed. If λ and z
11 are known and Λ is observed, then d can be calculated
12 using Eq. (1). In our configuration, the magnitude of
13 z varies depending on z-displacement from P_{ref}.

3. Results and Discussion

In the experiment, the feasibility of our system was
illustrated as follows. We generated double evanes-
cent illumination, on the prism surface (Fig. 1), with
the evanescent spots separated by a fixed distance of
$d = 1\,\mathrm{mm}$ [Fig. 2(a)]. In the far field, we observed

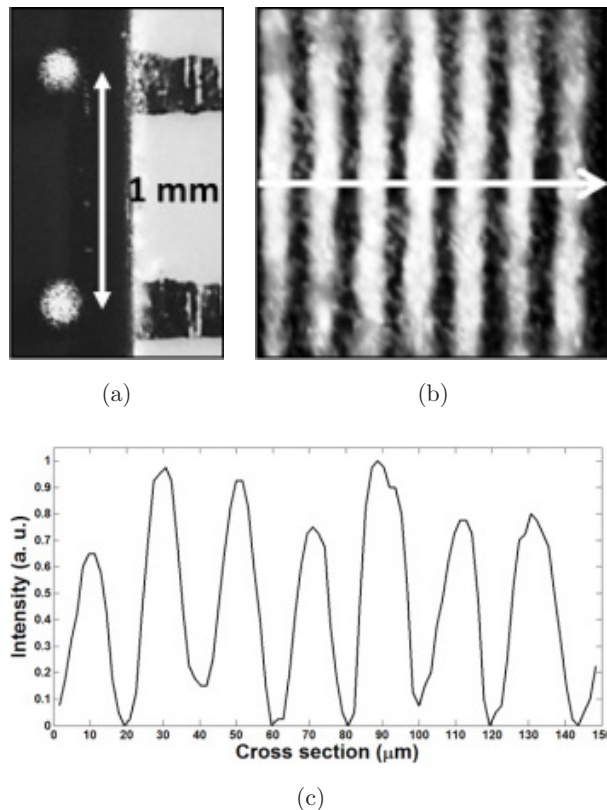(a)   (b)

(c)

Fig. 2. Double evanescent illumination (a) and their
interference pattern in the far-field radiation (b). Inter-
ference pattern cross-section (c) along the white arrow in (b).

clear interference fringes. A typical image
$(2048 \times 1536$ pixels) of the observed interference
pattern is presented in Fig. 2(b). The formation of
such fringes evidently suggests the transformation of
evanescent waves into (coherent) propagating com-
ponents via the interaction with small surface
defects. In order to have a qualitative analysis of such
pattern, first we evaluate the inter-fringe distance of
the observed image [Fig. 2(c)].

By analogy with the classic Young's experiment
with hard rectangular slits, the spots separation
distance can be estimated by using Eq. (1), where
$z = 33$ mm, $\lambda = 633\,\mathrm{nm}$, and $\Lambda = 21\,\mu\mathrm{m}$ represents
a typical experimental fringe period (Fig. 3) in this
configuration. This approximation yields separation
between spots of $d = 995\,\mu\mathrm{m}$. The pixel scale was
$1.615\,\mu\mathrm{m}$ per pixel and this value is used hereafter.
The agreement between the optical and the refer-
ence distance appears to be good. In the same con-
text, we imaged different separation distances, d,
which were experimentally fixed by means of dis-
tinct wire diameters [Figs. 4(a), 4(c) and 4(e)]. The
corresponding separation distance, d, is shown in
Figs. 4(a), 4(c) and 4(e) while Figs. 4(b), 4(d) and
4(f) shows the recorded pattern (at the same
z-distance) for each particular situation. We notice
good agreement between the optically estimated
values and those measured directly with measure-
ment precision instruments (Vernier) (Table 1).

The slightly different values of the wire diameters
are suspected to be due to our failure to exactly know
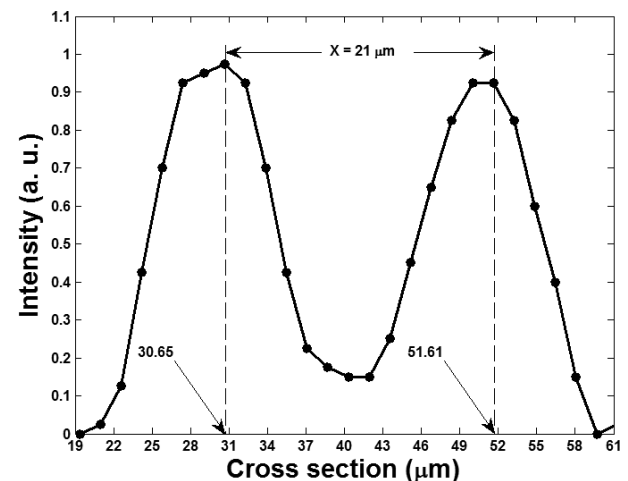the distance between P_{ref} and P_{obs}. On the other

Fig. 3.   Amplified portion of the cross-section in Fig. 2(c).

4   R. Cortes et al.

(a)   (b)

(c)   (d)

(e)   (f)
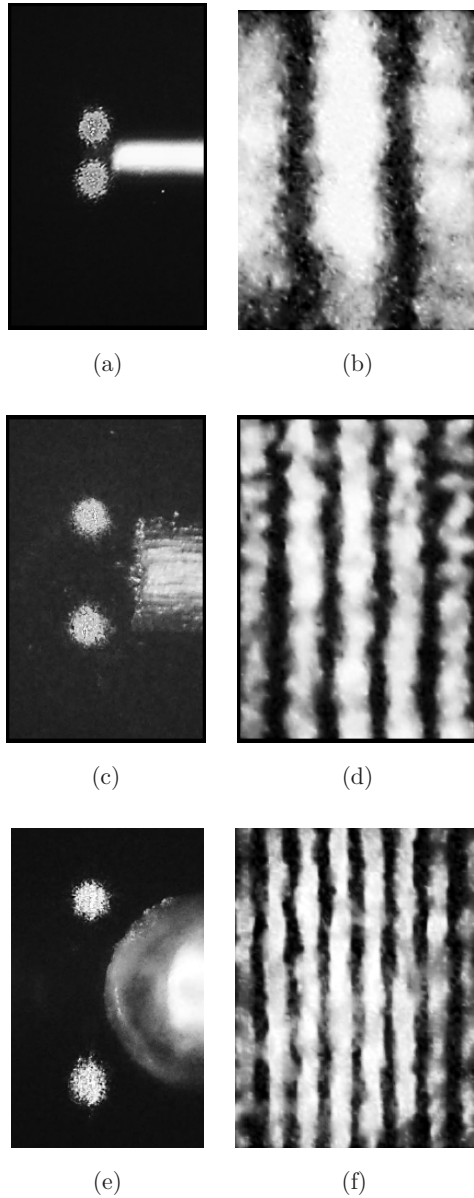
Fig. 4.   Double evanescent illumination with a separation distance of (a) 250 (b) 500 and (c) 900 μm and corresponding interference pattern in the far field with a period of (b) 79.4 μm (e) 37.7 μm and (f) 23.9 μm.

Table 1.   Optical measurement of the diameter of three different wires.

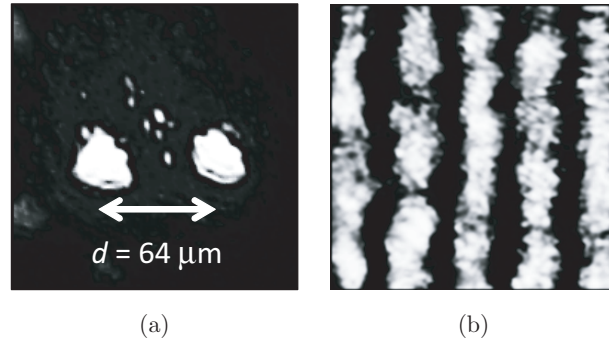| Λ (μm)	Diameter (Optically measured)	Diameter (Directly measured)
78.2	267 μm	250 μm
38.1	548 μm	500 μm
23.1	904 μm	950 μm

(a)   (b)

Fig. 5.   Pair of dust particles immersed in a single Gaussian evanescent illumination (a) and their far field interference pattern (b).

hand, we show the magnified detail of a single Gaussian evanescent spot with a pair of dust particles located at the spot centre [Fig. 5(a)].

Here, we observe the emission of coherent light, stemming from the dust particles under analysis, and the formation of an interference pattern that is still not complicated so that pronounced and clear fringes could be observed in the far field [Fig. 5(b)]. Thus, we estimated the separation distance of the dust particles using the same fringes analysis aforementioned. The separation distance of the dust particles was 64 μm [Fig. 5(a)] while the periodicity of the recorded pattern [Fig. 5(b)] was 123 μm. A last example is the diffraction pattern of a nearly circular small hole which is illuminated with a single Gaussian evanescent mode. The hole has a diameter of approximately 50 μm and is located in the mid-section of a thin aluminum foil, which is covering the prism surface. We use immersion oil ($n = 1.518$) to increase the efficiency of the scattered light between the air−aluminium interface. In Figs. 6(a) and 6(b), we show the diffraction pattern produced by the evanescent wave scattering through a circular aperture, recorded at two different positions along the optical axis. We can clearly see a Fresnel diffraction pattern [Fig. 6(a)], and a special spot known as Poisson spot [Fig. 6(b)]. This is expected because as the observation point moves away, the point at the center changes from constructive interference to destructive. Experimentally, the center point changes from bright to dark at 9 mm from the P_{ref} [Fig. 6(b)]. It changes again to a bright spot at 12 mm from the P_{ref} [Fig. 6(a)]. The irregularities of the fringes show that the hole was not
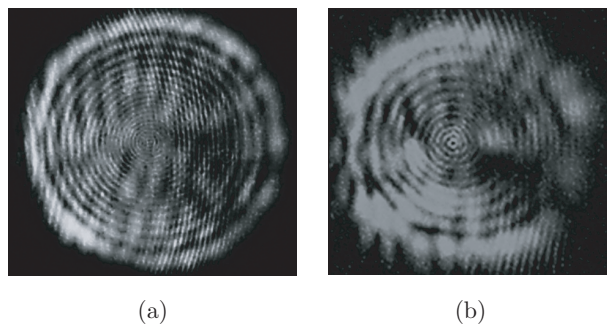
Fig. 6.   Diffraction patterns, resulting from the scattered field of an evanescent Gaussian illumination of a circular aperture, recorded at two different distances of z (a) 12 mm and (b) 9 mm. The images reproduce Fresnel diffraction patterns (a) and a spot known as Poisson's spot (b).

exactly circular. This experimental method is relatively simple to implement, however, one should bear in mind that from a mathematical point of view the near field diffraction integrals are difficult to perform.[10,18]

4.   Conclusion

Summarizing, we imaged interference and diffraction patterns in far field radiation when evanescent waves are transformed into (coherent) propagating components via the interaction with small surface defects. Using a simple setup, we demonstrate that it is possible to perform a direct visualization of evanescent wave phenomena as well as to carry out high accuracy spatial measurements. We have optically estimated the diameter of several wires and they are in a good agreement with the dimensions measured with high-precision mechanical instruments (Vernier). The functionality of our system, with individual (dust) particles immersed in a single Gaussian evanescent spot, was also corroborated. The results show the feasibility to measure (under proper conditions) inter-particle distances without using an external measurement instrument or advanced microscopes as for example atomic force microscopy. We also imaged diffraction patterns for a circular aperture where characteristic features as Fresnel diffraction pattern and Poisson spot were observed. The method is relatively simple to implement and can be also conceived as a tool for pedagogical purposes or in advanced research as for example surface plasmons polaritons phenomena.[19] In order to explore more its capacities further theoretical and experimental works are needed.

Acknowledgments

References

1. F. de Fornel, *Evanescent Waves: From Newtonian Optics to Atomic Optics* (Springer Heidelberg, 2001).
2. I. Newton, *Opticks* (Dover, New York, 1952).
3. Y. C. Shimabukuro, *The Essence of Dielectric Waveguides* (Springer, 2008).
4. F. M. Mirabella Jr., *Appl. Spectrosc. Rev.* **21** (1985) 45.
5. D. Courjon, *Near-Field Microscopy and Near-Field Optics* (Imperial College Press, 2003).
6. E. Wolf, *Opt. Lett.* **23** (1998) 16.
7. R. Quidant, J.-C. Weeber, A. Dereux, D. Peyrade, Y. Chen and C. Girard, *Europhys. Lett.* **57** (2002) 191.
8. A. B. Katrich, *Opt. Commun.* **255** (2005) 169.
9. E. A. Ray, M. J. Hampton and R. Lopez, *Opt. Lett.* **34** (2009) 2048.
10. K. G. Makris and D. Psaltis, *Opt. Commun.* **284** (2011) 1686.
11. T. W. Ebbesen, H. J. Lezec, H. F. Ghaemi, T. Thio and P. A. Wolff, *Nature* **391** (1998) 667.
12. D. A. B. Miller, *Opt. Lett.* **16** (1991) 1370.
13. F. Depasse, M. A. Paesler, D. Courjon and J. M. Vigoureux, *Opt. Lett.* **20** (1995) 234.
14. D. A. Papathanassoglou and B. Vohnsen, *Am. J. Phys.* **71** (2003) 670.
15. M. Xiao, R. Machorro and J. Siqueiros, *J. Vac. Sci. Technol. A* **16** (1998) 1420.
16. A. J. Meixner, M. A. Bopp and G. Tarrach, *Appl. Opt.* **33** (1994) 7995.
17. E. A. Bezus, L. L. Doskolovich and N. L. Kazanskiy, *Microelectron. Eng.* **88** (2011) 170.
18. A. C. Domínguez, J. B. Arroyo, J. E. G. Correa and G. M. Niconoff, *Rev. Mex. Fis. E* **56** (2010) 159.
19. V. Coello, *Surf. Rev. Lett.* **15** (2008) 867.